

Considerations regarding the Behaviour of X12CrMoS17 and X22CrNi17 Steels to the Cavitation Erosion

Assoc. Prof. PhD Eng. **Lavinia Mădălina MICU**¹, Prof. PhD Eng. **Ilare BORDEAȘU**^{2,3},
Assoc. Prof. PhD Eng. **Daniel OSTOIA**², Dipl. Eng. **Robert PARMANCHE**²,
Assist. Prof. PhD Eng. **Alexandru Nicolae LUCA**², Lect. PhD Eng. **Cristian GHERA**^{2,*},
Lect. PhD Eng. **Corneliu Eusebiu PODOLEANU**⁴, Lect. PhD Eng. **Cornelia Laura SĂLCIANU**⁵

¹ Department of Agricultural Technologies-Department I, King Mihai I University of Life Sciences, Timisoara, Romania

² Department of Mechanical Machines, Equipment and Transportation, University Politehnica of Timisoara, 2 Piata Victoriei, 300006 Timisoara, Romania

³ Romania Academy of Scientists, Timisoara Branch, Mihai Viteazul str. no.1, Timisoara, Romania

⁴ Department of Hydrotechnical Engineering, University Politehnica of Timisoara, 2 Piata Victoriei, 300006 Timisoara, Romania

⁵ Department of Mechantronics, University Politehnica of Timisoara, 2 Piata Victoriei, 300006 Timisoara, Romania

* cghera2000@yahoo.com

Abstract: *The paper presents the results of the cavitation erosion research carried out on two stainless steels intended for the manufacture of parts strongly subjected to cavitation, such as the vanes and rotors of hydraulic turbines and pumps. In accordance with the new trends, to reduce carbon below 0.1%, for both categories the carbon content was kept at the value of 0.038%. The researches are carried out in the Cavitation Erosion Research Laboratory of the Politehnica University of Timisoara, on the magnetostrictive vibrating device with a nickel tube. The behaviour and resistance to cavitation erosion are evaluated based on the comparison of curves and specific parameters with those of OH12NDL stainless steel, as a reference for the parts subjected to cavitation, as well as on the basis of microstructural images, obtained by optical and electron microscopy. The results show similarities and differences of microstructural damage between the two steels. The comparison of the specific curves and the values of the reference parameters, with those of the reference steel OH12NDL, shows that both steels can be successfully used in the manufacture of vanes and rotors of hydraulic machines.*

Keywords: *Cavitation erosion, specific curves, microstructural constituents*

1. Introduction

The destruction caused by cavitation erosion, especially in the rotors of turbines and hydraulic pumps, led researchers to continue studies on the destruction [1-12] and to look for new materials with high resistance to this phenomenon. In the same direction, the research presented in the paper, carried out in the Cavitation Erosion Research Laboratory in Timișoara on two categories of stainless steels, with identical carbon contents (0.038%), different chromium contents (15.8%, respectively 11.302 %) and nickel (3.051 % and 4.236 %). The study of the two categories of steels, produced in Romania, was determined by the erosive problems found in the vanes and rotors of the turbines of the hydroelectric power plants in Romania, which were undergoing refurbishment.

2. Researched materials

The experimental steels were procured from UCM Resita. Their chemical composition is presented in table 1 and was determined using a Foundry Master spark optical emission spectrometer, manufactured by WAS (Germany), in the equipment of the Spectrochemical Experiments Laboratory of Optical Emission and X-ray Fluorescence, within the Center of Special Materials Expertise (CEMS) from the National University of Science and Technology Politehnica Bucharest. The microstructural constitutions and approximate proportions, shown in table 2, were determined

using the Schäßler diagram, figure 1, based on the equivalent coefficients in chromium (Cr)_e and nickel (Ni)_e calculated with the relation [6]:

$$(\text{Cr})_e = \% \text{Cr} + 1.5\% \text{Si} + \% \text{Mo} + 0.5\% (\text{Ta} + \text{Nb}) + 2\% \text{Ti} + \% \text{W} + \% \text{V} + \% \text{Al}$$

(1)

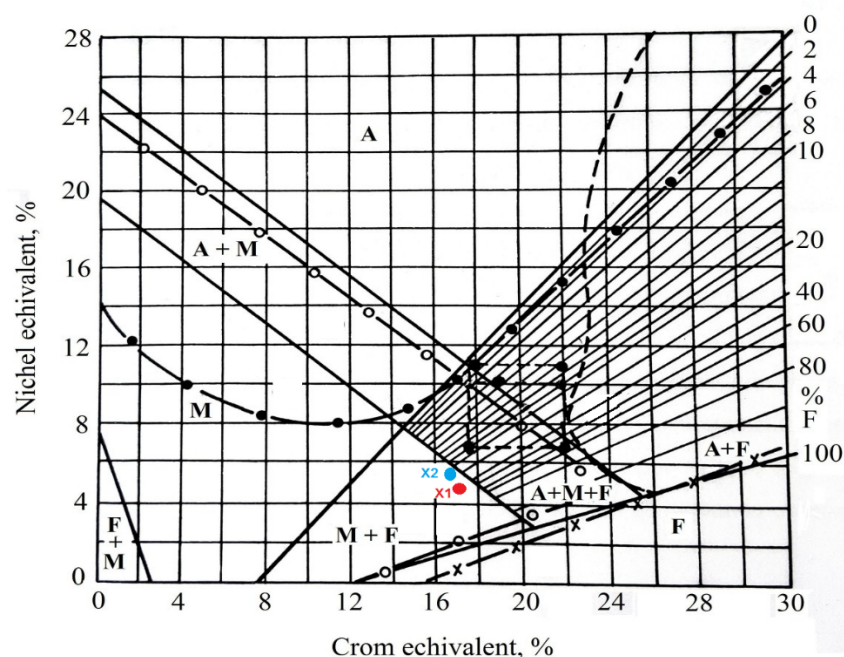
$$(\text{Ni})_e = \% \text{Ni} + 3\% \text{C} + 0.5\% \text{Mn} + 0.5\% \text{Co}$$

Table 1: Chemical composition of experimental stainless steels

Steel (Symbolization)								
	C	Si	Mn	P	S	Cr	Mo	Ni
X12CrMoS17 (X1)	0.038	1.15	3.13	0.007	0.016	15.80	2.59	3.051
X22CrNi17 (X2)	0.038	1.16	2.12	0.007	0.016	11.302	1.69	4.236

Table 2: Prediction of the microstructural constitution according to the Schäßler diagram

Steel	(Cr) _e	(Ni) _e	≅ Martensite %	≅ Ferrite %
X1	17.213	4.73	60	40
X2	16.8	5.41	70	30

**Fig. 1.** Positioning of the two steels in the Schaeffler diagram

The microstructure of the two experimental stainless steels, shown in figure 2a, was performed with the Reichert metallographic microscope. The microstructural analysis is in accordance with the data established on the basis of the Schäßler diagram; steels having close casting structures, with relatively fine graining. Both steels have fine acicular martensite as their major constituent, to which is added ferrite, with island arrangement, in different proportions (see table 2).

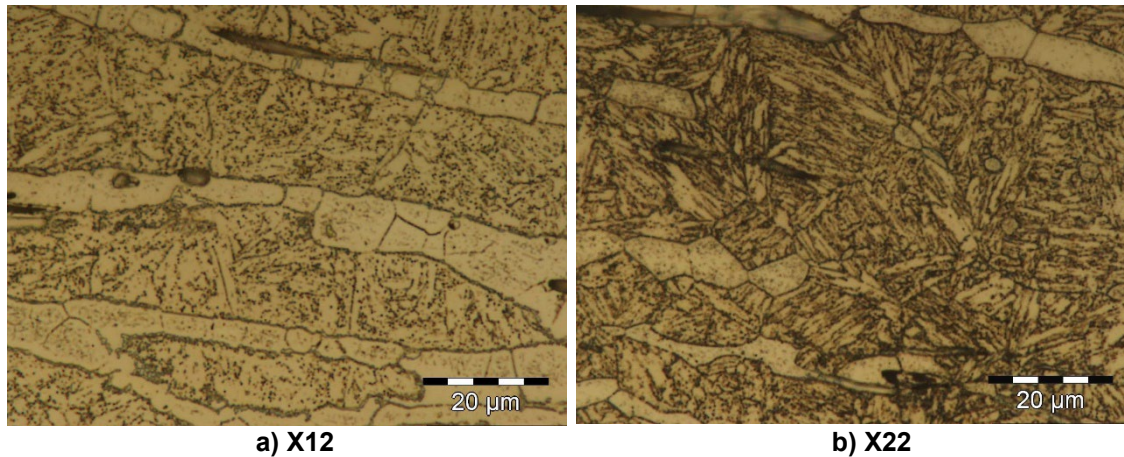


Fig. 2. The microstructural aspect of experimental stainless steels, 1000 x (attack glycerine royal water).

3. Method and apparatus used

The cavitation erosion tests were performed on the magnetostrictive vibrator with a nickel tube, figure 3, respecting the laboratory's custom [5, 6, 11-16] and the requirements of the international standards ASTM G32-2016 [14]. The operating parameters of the device were [6, 13]:

- power = 500 W
- vibration frequency $7000 \pm 3 \%$ Hz
- double vibration amplitude = 94 μm
- sample diameter = 14 mm, fig.3.b
- sample type = vibration.

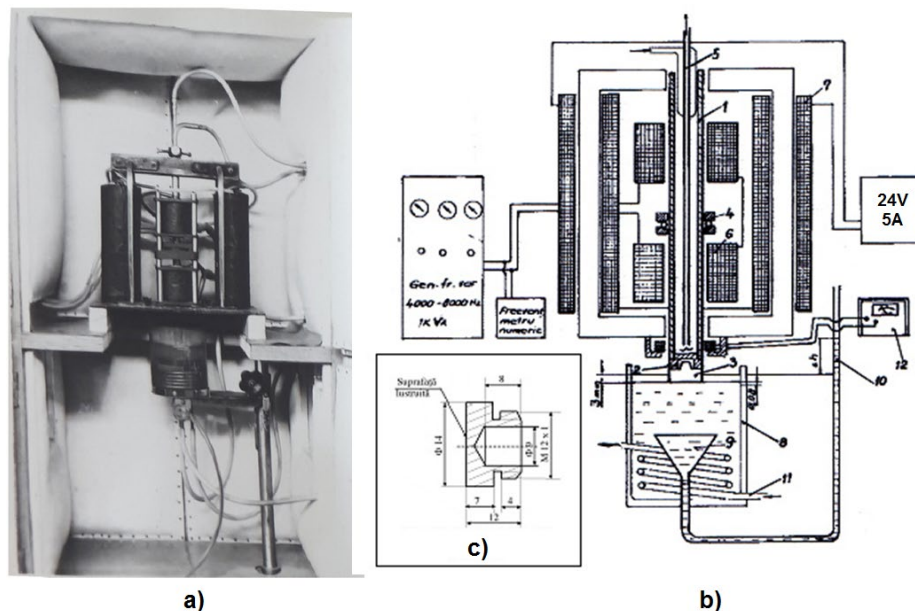


Fig. 3. The magnetostrictive vibrator (elaboration from [6, 13]):

- a) device image, b) principle diagram, c) geometric shape of the sample
 (1- nickel tube; 2 - part - sample fixation; 3 - sample; 4 - nickel tube fixation ring system;
 5 - nickel tube cooling system; 6 - alternating current coils; 7 - direct current coils;
 8 - liquid container work; 9 - sonic wave capture; 11 - cooling coil (voltammeter))

The liquid medium used was double-distilled water, the temperature of which was kept constant throughout the tests at 22 ± 1 °C. The total duration of the cavitation tests, according to the procedures of our cavitation laboratory [11-13, 15, 16], was 165 minutes, divided into 12

intermediate periods (each of 5 and 10 minutes and 10 of 15 minutes). At the beginning and end of each test period, the samples were successively washed in tap water, double distilled water, alcohol and acetone and then weighed.

The preservation of each sample, during the breaks between test periods, was done in desiccators to avoid the possible influence of environmental factors that could affect the structure subject to cavitation erosion.

For rigor, were tested three samples of each material. The results presented in the paper, through the curves and specific parameters, are averages of the experimental values determined on the three samples.

After finishing the tests, the samples were subjected to structural analyses, both in the plane of the surface exposed to cavitation, and in the axial section, perpendicular to the cavitation surface, to measure the maximum penetration depth of the cavitation. For the analysis of the degradation of the structure and how it correlates with the experimental results of the cavitation test, the images recorded with the optical stereomicroscope OLYMPUS SZX 7, equipped with the image processing program, quick Micro photo 2.2, and those of to the scanning electron microscope type XL-30-ESEM TMP, both microscopes are in the CEMS equipment of the National University of Science and Technology Politehnica Bucharest.

4. Experimental results

Based on the mass losses, recorded at the end of each attack period, the curves of the cumulative mass losses, figure 4 and of the erosion velocities, figure 5, were built. The mass losses and the erosion velocities, from the two figures, are algebraic averages of the obtained values on the three samples, tested from each type of steel.

To evaluate the strength and behaviour during the attack, the curves of the reference steel for the reference steel OH12NDL (0.1% C, 12.8% Cr, 1.25% Ni, 74% martensite, 26% ferrite) were also represented in the same diagrams.

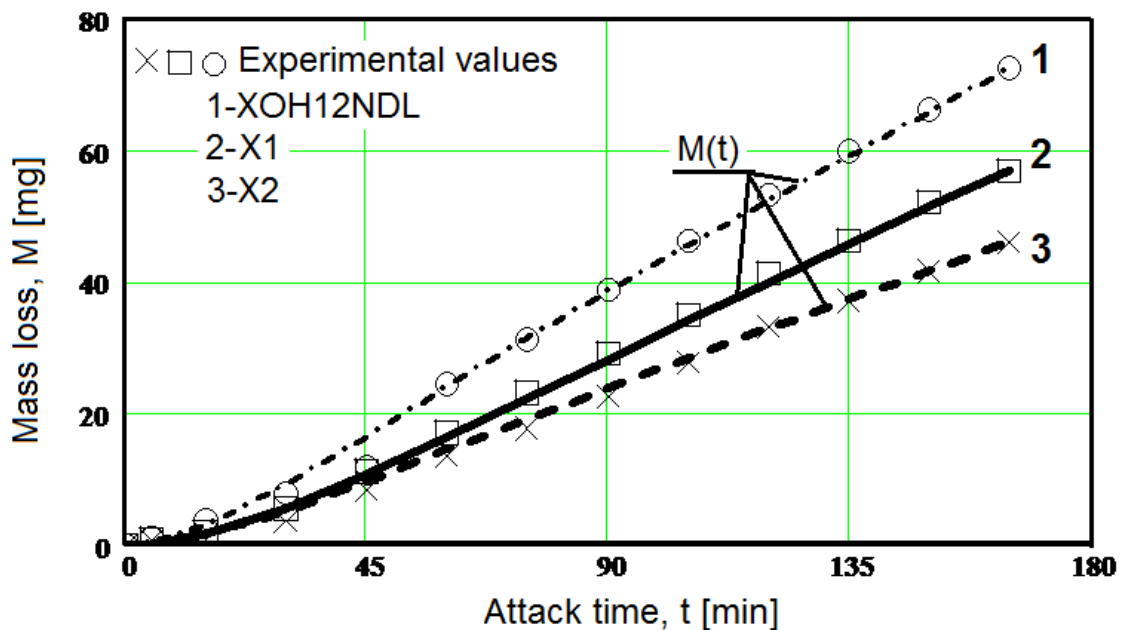


Fig. 4. The variation of the cumulative mass losses with the duration of the cavitation attack (comparison with the reference steel OH12NDL)

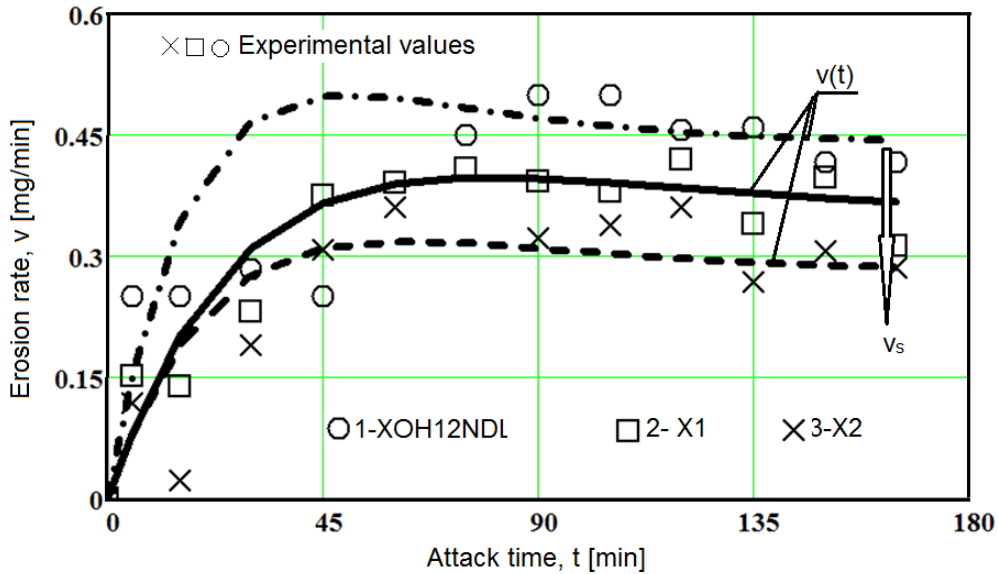
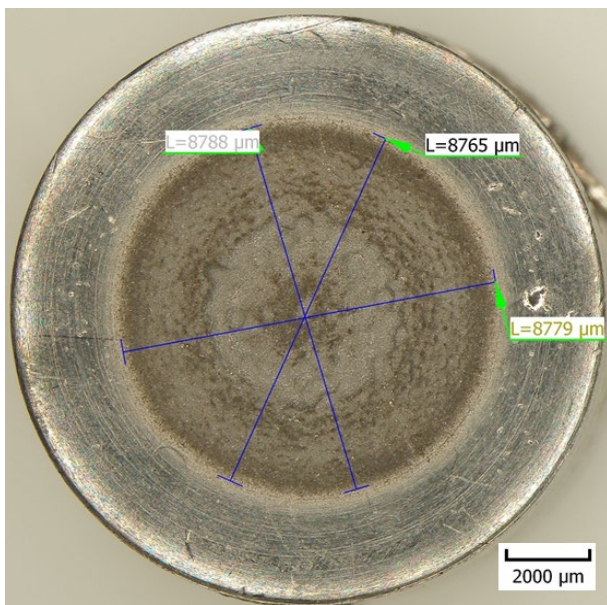
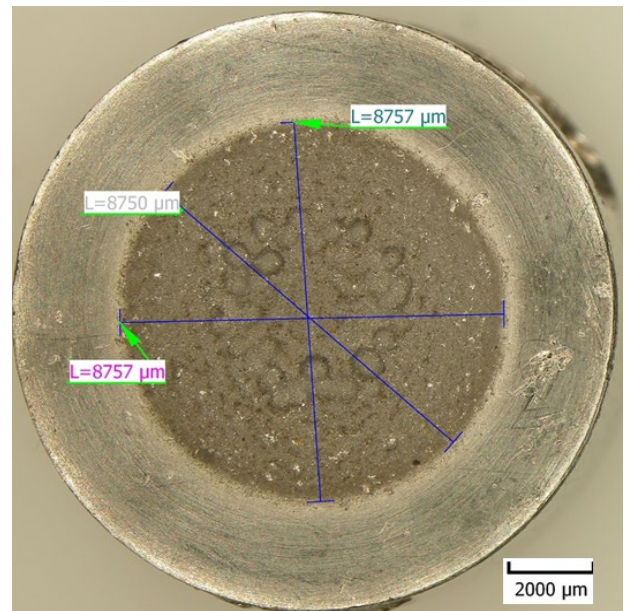


Fig. 5. The variation of the erosion rate with the duration of the cavitation attack (comparison with the reference steel OH12NDL)

The macrostructural image of the cavity surface, figure 6, is obtained by stereomicroscopy. This highlights the aspects of the surfaces affected by erosion, and comparatively, the differences between their average diameters. It is noted that the affected surfaces have relatively inhomogeneous aspects in both steels and, compared to the exposed surface with a diameter of 14 mm, they are between 40.91% (for steel X1) and 40.70% (for steel X2). The maximum cavitation penetration depth (see figure 7) was determined after sectioning the test samples, with values ranging from 958 μm (for steel X1) to 675 μm (for steel X2).



The average diameter of the affected surface = 8777 μm
 The percentage of the surface affected by cavitation = 40.91%
a) Steel X1



The average diameter of the affected surface = 8754 μm
 The percentage of the surface affected by cavitation = 40.70 %
b) Steel X2

Fig. 6. The stereomicrostructural aspect of the samples, highlighting the area affected by the cavitation

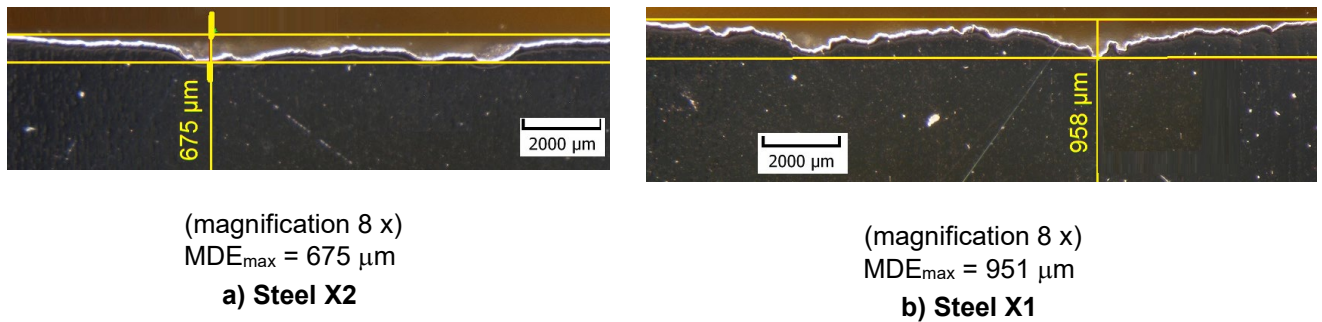


Fig. 7. The maximum depths of the erosions from the experimental samples (stereomicroscope images)

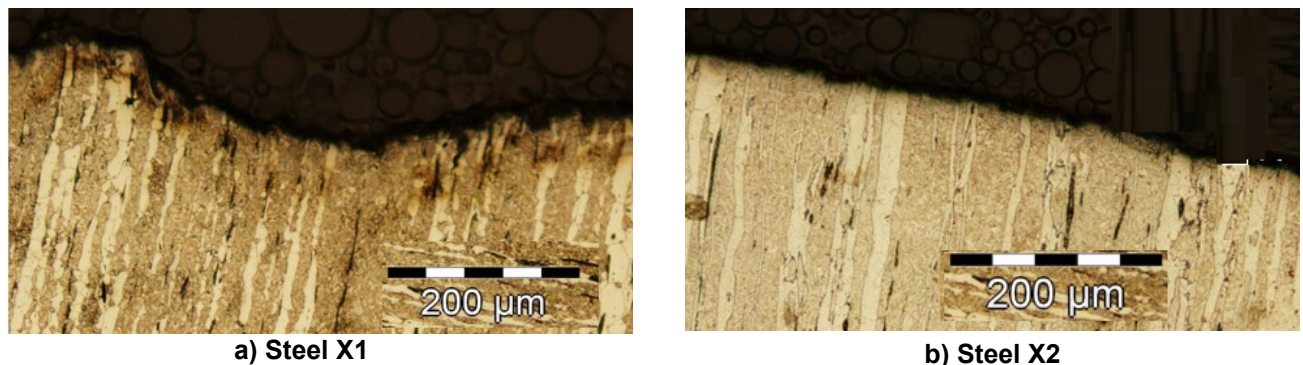


Fig. 8. Aspects of the microstructural destruction, highlighting the hardening in the area bordering the erosion (metallographic attack glycerine royal water, 100 x)

The images in figure 8 show the destruction at the microstructural level with a hardened zone in the boundary layer of the destroyed zone under the repeated impact of microjets and shock waves produced by the implosion of cavitation bubbles [6, 7, 13, 11, 12, 15, 17-20].

5. Results analysis. Discussions

Analysis of results based on characteristic curves and fractographic images

The data from the diagrams, from fig.4 and fig.5, related to the characteristic curves of the reference steel OH12NDL, show that the studied steels have a very good cavitation behaviour. From the comparison of the curves of the two steels, it follows that the X2 steel (with 70% martensite) has an advantage in cavitation resistance. We believe that this increase is due to the higher content of martensite, the constituent with the highest resistance to cavitation [1, 2, 11, 12, 15]. The higher resistance of the X2 steel is also determined by the somewhat finer structure, determined by the lower amount of Mn, which contributes to the increase in the size of the crystalline grains.

The dispersion of the experimental values compared to the approximation curves is the consequence of the grain sizes, resulting from casting and expelled during the cavitation attack. This dispersion is also supported by the images of the profiles of the eroded areas in figure 7 (through the maximum depth of penetration) and figure 8.

The images in figure 7 show that the maximum bending depth, measured at the end of the tests, differs from one steel to another and agrees with the evolution of the specific curves. Also, the results obtained in the Cavitation Laboratory [6, 11-13, 15, 16], show that this depth depends on the sizes of the crystalline grains and is not suitable for comparing materials. Eventually, it can be used to assess the cavity behaviour based on the drilling technology.

The results from the Cavitation Laboratory and made public [6, 11-13, 15, 16] obtained in over 60 years of research in the field, lead us to affirm that the mean depth of erosion (MDE_{max}), obtained

by calculation from the total mass cumulative [6, 11, 13] is an indicated parameter in the comparison of cavity erosion resistance.

In the images in figure 7, it is also possible to see a very small area, near the eroded area, where a local deformation of the material can be distinguished, which is an effect of the intensity of cavitation, respectively the repetitive impact of the material with shock waves and microjets generated by the implosion of cavitation bubbles [6, 13].

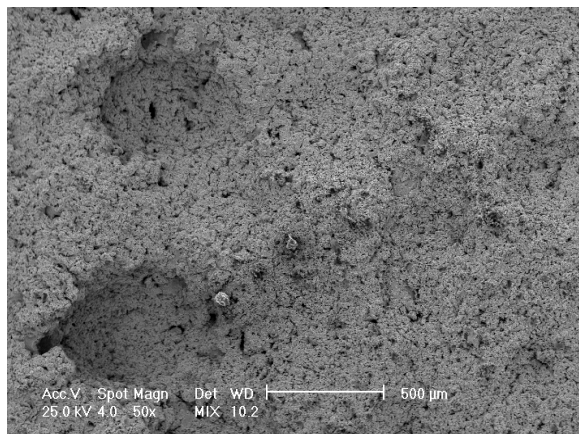
The analysis carried out by electron microscopy (SEM), figure 9, highlights the following evolutions of the damages produced at the microstructural level:

1. Steel X1:

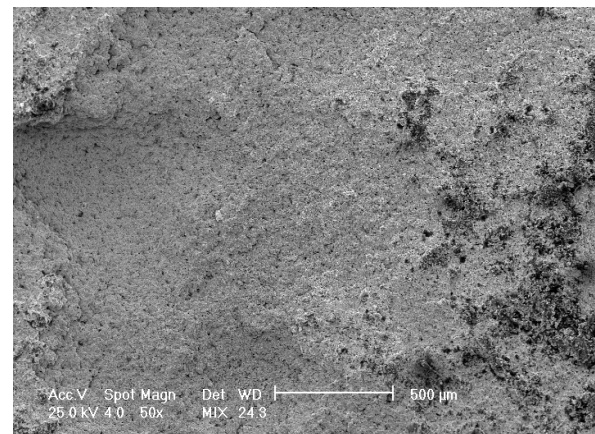
- fracture through cavity with intergranular, brittle aspect,
- mixed appearance with very large cavities (200-500 μm) and fine cavities up to 15 μm ,
- breaking with a brittle appearance with the highlighting of intergranular cracks,
- areas of fracture propagation through cleavage and fine gaps up to 10 μm .

2. Steel X2:

- fine cavities of 10-15 μm and numerous microvoids evenly distributed on the surface,
- fine intergranular cracks and mixed appearance of the fracture with cleavage zones,
- brittle fracture with intergranular propagation with cleavage zones.



a) Steel X1



b) Steel X2

Fig. 9. SEM image of the cavitated surface (100x)

Table 3 shows the values v_s towards which the $v(t)$ curves tend to stabilize, specific to the cavitation resistance of the two investigated steels, as well as the normalized resistance, R_{ns} , which takes into account the cavitation resistance of the reference steel OH12NDL, by the value of its stabilization speed, $V_{s \text{ OH12NDL}}$.

Table 3: Comparison of cavitation erosion resistance with that of the reference steel OH12NDL

Parameter	X1	X2
v_s [mg/min]	0.37	0.29
$R_{ns} = v_{s \text{ oțel}} / v_{s \text{ OH12NDL}}$	0.84	0.66

The data in table 3 confirm the analyses carried out based on the curves in fig. 4 and fig.5, highlighting the anti-cavitation qualities of the investigated steels.

Therefore, we appreciate that the two steels, with different contents of chromium and nickel, with different microstructures, have different behaviour/resistance to cavitation. The practical problem that arises for the two steels is that they allow the welding operations to be carried out, which is done during the repair periods, with the aim of extending the lifetime of the vanes and rotors [6].

6. Conclusions

1. The investigated steels show very good cavitation erosion behaviour, superior to the reference steel OH12NDL and recommend them in the manufacture of vanes and rotors of hydraulic machines.
2. The creation of steels, based on the criteria of controlled chromium and nickel contents, with low carbon content (below 0.1 %) offers the advantage of deeper analyses of the behaviour of materials in cavitation, highlighting the common and different elements of the destruction evolution.
3. We appreciate that the maximum depth of erosion, measured at the end of the research, fig. 6, being dependent on the size of the expelled grains, is not suitable for comparison with other materials. The agreement of its dimensions with the evolution of the behaviour of the two steels, in the analysed case, is purely coincidental. Eventually, it can be used to assess the cavitation behaviour based on the manufacturing technology. The parameter recommended by us is the average penetration depth, calculated based on the volume of eroded material.

References

- [1] Bordeasu, D., O. Prostean, I. Filip, F. Dragan, and C. Vasar. “Modelling, Simulation and Controlling of a Multi-Pump System with Water Storage Powered by a Fluctuating and Intermittent Power Source.” *Mathematics* 10, no. 21 (2022): 4019.
- [2] Bordeasu, D., O. Proștean, and C. Hatiegan. “Contributions to Modeling, Simulation and Controlling of a Pumping System Powered by a Wind Energy Conversion System.” *Energies* 14, no. 22 (2021): 7696.
- [3] Bordeasu, D. “Study on the implementation of an alternative solution to the current irrigation system.” *Acta Technica Napocensis Series Applied Mathematics, Mechanics and Engineering - Special Issue* 65, no. 3 (2022): 593-602.
- [4] Bordeasu, D., F. Dragan, I. Filip, I. Szeidert, and G. O. Tirian. “Estimation of Centrifugal Pump Efficiency at Variable Frequency for Irrigation Systems.” *Sustainability* 16, no. 10 (2024): 4134.
- [5] Bordeasu, I., M. O. Popoviciu, V. Balasoiu, A. D. Jurchela, and A. Karabenciov. “Influence of the vibratory test facility type and parameters upon the cavitation erosion evolution.” Paper presented at the 25th IAHR Symposium on Hydraulic Machinery and Systems, Timisoara, Romania, September 20-24, 2010. *IOP Conference Series: Earth and Environmental Science* 12 (2010): 012037.
- [6] Bordeasu, I. *Cavitation erosion of materials / Eroziunea cavitațională a materialelor*. Timișoara, Politehnica Publishing House, 2006.
- [7] Heathcock, C. J., B. E. Protheroe, and A. Ball. “Cavitation erosion of stainless steels.” *Wear* 81, no. 2, (October 1982): 311-327.
- [8] Hattori, S., and T. Kitagawa. “Analysis of cavitation erosion resistance of cast iron and nonferrous metals based on database and comparison with carbon steel data.” *Wear* 269, no. 5-6 (July 2010): 443-448.
- [9] Hattori, S., N. Mikami. “Cavitation erosion resistance of stellite alloy weld overlays.” *Wear* 267, no. 11, (October 2009): 1954-1960.
- [10] Hattori, S., and R. Ishikura. “Revision of cavitation erosion database and analysis of stainless steel.” *Wear* 268, no. 1-2 (2010): 109-116.
- [11] Micu, L. M., I. Bordeasu, M. O. Popoviciu, M. Popescu, D. Bordeasu, and L. C. Salcianu. “Influence of volumic heat treatments upon cavitation erosion resistance of duplex X2CrNiMoN 22-5-3 stainless steels.” Paper presented at the International Conference on Applied Sciences 2014 (ICAS 2014), Hunedoara, Romania, October 2-4, 2014. *IOP Conference Series: Materials Science and Engineering* 85 (2015): 012019.
- [12] Bordeasu, I., M. O. Popoviciu, I. Mitelea, L. C. Salcianu, D. Bordeasu, S. T. Duma, and A. Iosif. “Researches upon the cavitation erosion behaviour of austenite steels.” Paper presented at the International Conference on Applied Sciences 2015 (ICAS 2015), Wuhan, China, June 3–5, 2015. *IOP Conference Series: Materials Science and Engineering* 106 (2016): 012001.
- [13] Bordeasu, I. *Monograph of the Cavitation Erosion Research Laboratory of the Polytechnic University of Timisoara (1960-2020) / Monografia Laboratorului de Cercetare a Eroziunii prin Cavitație al Universității Politehnica Timișoara (1960 – 2020)*. Timișoara, Politehnica Publishing House, 2020.
- [14] ASTM International. “ASTM G32 - 16: Standard Test Method for Cavitation Erosion Using Vibratory Apparatus”, 2016.
- [15] Bordeasu, I., M. O. Popoviciu, L. M. Micu, O. V. Oanca, D. Bordeasu, A. Pugna, and C. Bordeasu. “Laser beam treatment effect on AMPCO M4 bronze cavitation erosion resistance.” Paper presented at the International Conference on Applied Sciences 2014 (ICAS 2014), Hunedoara, Romania, October 2-4, 2014. *IOP Conference Series: Materials Science and Engineering* 85 (2015): 012005.

- [16] Popoviciu, M. O., and I. Bordeasu. “Considerations Regarding the Total Duration of Vibratory Cavitation Erosion Test.” Paper presented at the Third International Symposium on Cavitation, Grenoble, France, April 7-10, 1998.
- [17] Franc, J. P., and J. M. Michel. *Fundamentals of Cavitation*. Dordrecht, Kluwer Academic Publishers, 2004.
- [18] Chiu, K. Y., F. T. Cheng, and H. C. Man. “Cavitation erosion resistance of AISI 316L stainless steel laser surface-modified with NiTi.” *Materials Science and Engineering: A* 392, no. 1-2 (February 2005): 348-358.
- [19] Hammitt, F. G., M. De, J. He, T. Okada, and B.-H. Sun. “Scale Effects of Cavitation Including Damage Scale Effects.” Paper presented at the 19th American Towing Tank Conference, Ann Arbor, Michigan, USA, July 9–11, 1980.
- [20] Franc, J. P., F. Avellan, B. Belhadji, J. Y. Billiard, L. Briancon-Marjollet, D. Frechou, D. H. Fruman, A. Karimi, J. L. Kueny, and J. M. Michel. *Cavitation. Physical Mechanisms and Industrial Aspects / La Cavitation. Mécanismes Physiques et Aspects Industriels*. EDP Sciences, Les Ulis Cedex, 1995.
- [21] Di V. Cuppari, M. G., R. M. Souza, and A. Sinatora. “Effect of hard second phase on cavitation erosion of Fe–Cr–Ni–C alloys.” *Wear* 258, no. 1-4 (January 2005): 596–603.